the spectrum is essentially decoupled for $N = 89$–91, intermediate for $N = 93$ and strongly coupled for $N = 95, 97$. Note, however, that also for these latter isotopes the high spin favoured states, $I = 17/2, 21/2, 25/2, \ldots$ come relatively lower in energy than the unfavoured $15/2, 19/2, 23/2$ states. Thus, as expected, the rotation aligned coupling scheme becomes more important with increasing spin.

Here we have only discussed the two extreme coupling schemes. It should, however, be evident that it is straightforward to diagonalise the full particle–rotor Hamiltonian and thus to describe intermediate situations as for example the spectra of ^{161}Er and ^{163}Er shown in fig. 11.9. Furthermore, only axially symmetric shapes have been considered. For the generalisation of the particle–rotor Hamiltonian to non-axial shapes, we refer to Larsson, Leander and Ragnarsson (1978) for a derivation along the lines presented here or to Meyer-ter-Vehn (1975) for a somewhat different derivation.

11.3 Two-particle excitations and back-bending

The collective angular momentum vector, **R**, is built from small contributions of all the paired nucleons. None of the wave functions is then strongly disturbed. For particles in low-Ω high-j orbitals one must, however, expect tendencies, not only for odd nucleons but also for paired nucleons, to align their spin vectors along the collective spin vector (Stephens and Simon, 1972). The maximal aligned spin for the two nucleons in a pure j-shell is then $\alpha_1 = j$ and $\alpha_2 = j - 1$, respectively, leading to a total aligned spin of $\alpha = \alpha_1 + \alpha_2 = 2j - 1$. With $R = I - \alpha$, the collective rotational energy is given by (cf. preceding section):

$$E_{\text{rot}} = \frac{\hbar^2}{2\mathscr{J}} R(R+1) = \frac{\hbar^2}{2\mathscr{J}} (I-\alpha)(I-\alpha+1)$$

The alignment is however accompanied by the breaking of one pair leading to a configuration with 'two odd particles'. A rough estimate is therefore that the energy cost for breaking the pairs is approximately twice the odd–even mass difference, 2Δ (see chapter 14). Compared to this, the energy cost for redistributing the particle wave function over the different orbitals, as discussed in the preceding section, can be neglected. Furthermore, the pairing correlations will tend to decrease this energy.

In the present approximation, we thus get for the band with 'two aligned spins'

$$E \approx 2\Delta + \frac{\hbar^2}{2\mathscr{J}} (I-\alpha)(I-\alpha+1); \quad I \geq \alpha$$

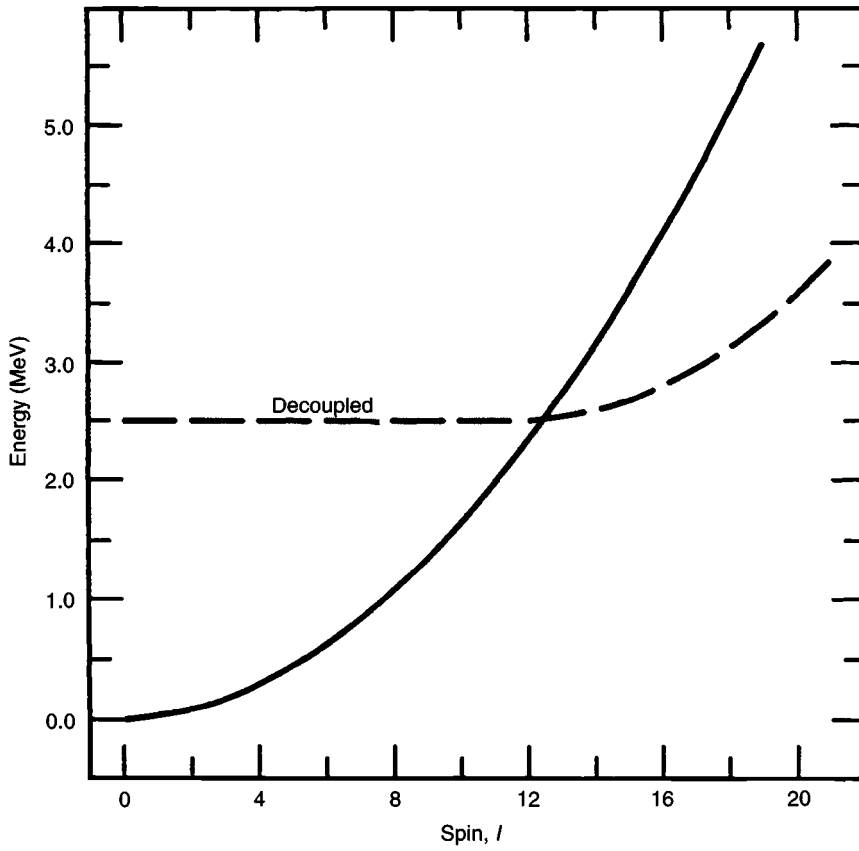

Fig. 11.10. Simple estimates are shown of the ground-band energy in an even–even $A \simeq 160$ nucleus (solid line) and the energy of a decoupled band based on two 'aligned' $i_{13/2}$ particles (dashed line) (from F.S. Stephens, *Proc. 4th Summer School on Nuclear Physics*, Rudziska, Poland, 1972, p. 190).

Total spin values smaller than the largest possible aligned spin can be obtained by a partial alignment with no collective rotation. Provided one pair is broken, this should lead to an energy $E \approx 2\Delta$. The resulting 'aligned' band is compared with the ground band in fig. 11.10.

The states having lowest possible energy for given spin are referred to as the yrast states. A typical yrast line for an $A \simeq 160$ nucleus is sketched in fig. 11.11. In this figure is also shown how the yrast levels can be studied. If two nuclei, e.g. $^{40}_{18}Ar_{22}$ and $^{124}_{52}Te_{72}$ collide in a non-central collision, a compound nucleus having a large excitation energy and a large angular momentum might be formed. By emission of e.g. four neutrons, which each carry away about 8 MeV of excitation energy (i.e. the neutron binding energy) a point some few MeV above the yrast line is reached.

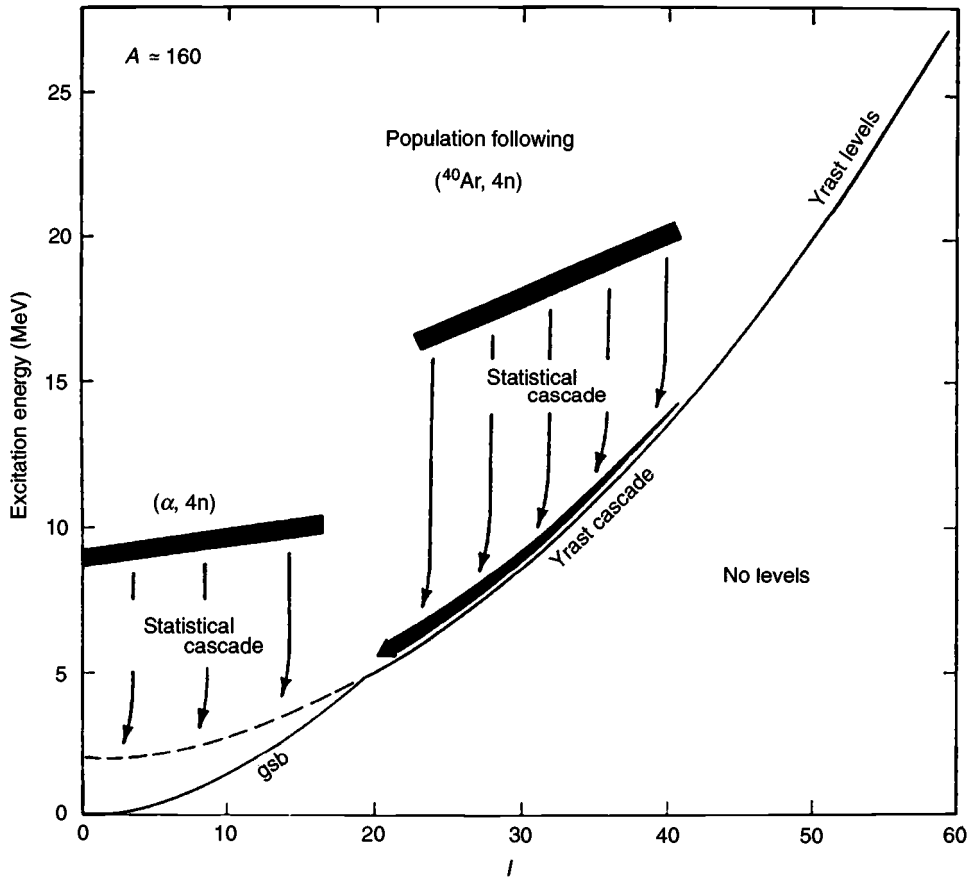

Fig. 11.11. Schematic illustration of which nuclear states are populated in reactions where either ^{40}Ar or an α-particle fuses with a target nucleus to form a compound system with $A \simeq 160$. Such reactions are best suited for the study of the yrast states, i.e. the lowest energy states for each spin I (partly from Stephens and Simon, 1972).

Some additional excitation energy might be carried away by a few so called statistical γ-rays and the yrast region is reached. The additional excitation energy is now carried by the rotational motion. For collective rotation, the compound nucleus will now de-excite mainly through E2 transitions, $(I+2) \rightarrow I$, along the yrast line. A situation like in fig. 11.10 will then lead to E2 energies that are larger for spins $I = 8$–10 than for spins $I = 14$–16.

In fig. 11.11 is also illustrated that the real high spin states can only be reached in so called heavy-ion collisions where both the projectile and the target are heavy nuclei. If an α-particle is used as projectile, only lower spin states can be reached (see problem 11.4).

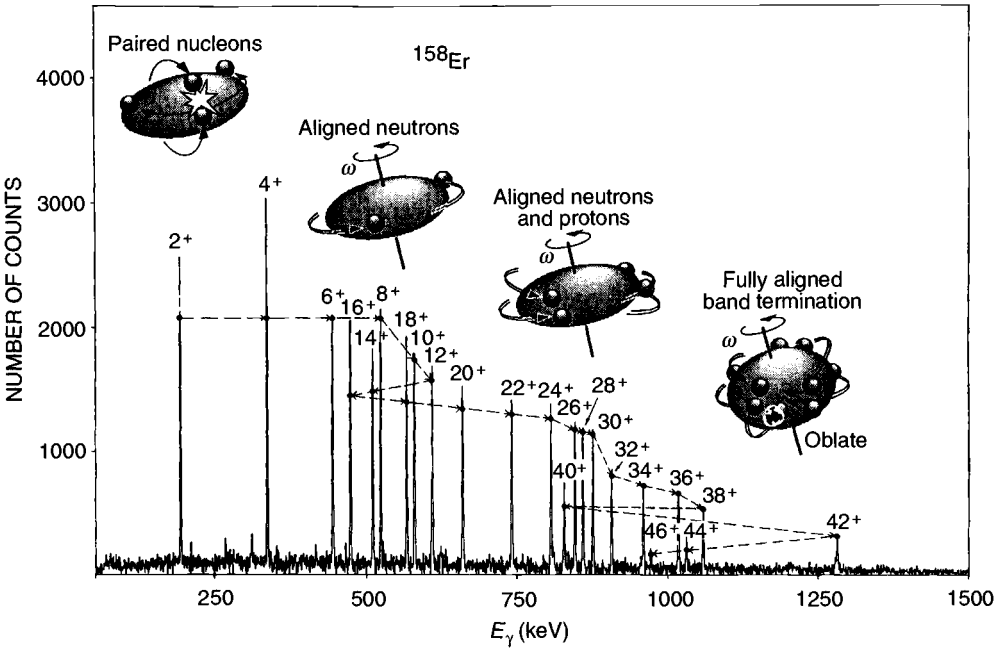

Fig. 11.12. Observed γ-ray energies of ^{158}Er formed in a reaction like the one illustrated in fig. 11.11. For $I \approx 14$ two $i_{13/2}$ neutrons become aligned resulting in a backbend while a second irregularity caused by the alignment of two $h_{11/2}$ protons is seen for $I \approx 32$. The features for $I \geq 38$ with the final band termination for $I = 46$ are discussed in chapter 12.

As seen in fig. 11.12, the experimentally observed E2 energies of ^{158}Er in the range $I = 12$–18 show the properties expected from the simple model of fig. 11.10. Of course, one must expect that the ground band and the decoupled band interact in the crossing region giving rise to a smoother transition between the two bands than shown in fig. 11.10. This is in agreement with the experimental spectrum of ^{158}Er. We must also remember that the model we have described is very much idealised. Still it seems to contain the main features of the physical effect.

The feature that the yrast E2 transition energies suddenly become smaller with increasing spin is generally referred to as back-bending (see fig. 11.12). When investigating such spectra, the yrast energies are often plotted in a somewhat different way. An effective moment of inertia as a function of the spin I can be obtained as

$$\frac{2\mathcal{J}}{\hbar^2} = \left(\frac{\mathrm{d}E}{\mathrm{d}I(I+1)}\right)^{-1} \simeq \left(\frac{E_I - E_{I-2}}{4I-2}\right)^{-1}$$

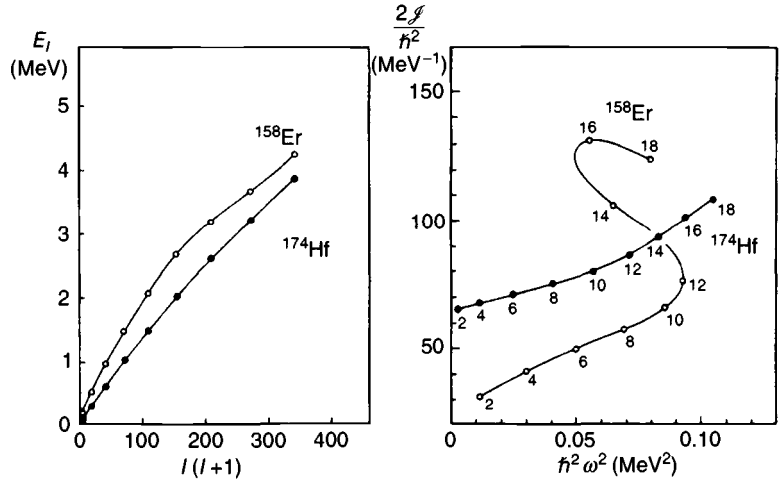

Fig. 11.13. Yrast energies in the $I = 0$–18 range of ^{158}Er and ^{174}Hf plotted versus $I(I+1)$ and corresponding back-bending plots with the moment of inertia $\mathcal{J}$ versus the squared rotational frequency, ω^2 (from R.M. Lieder and H. Ryde, *Adv. in Nucl. Phys.*, eds. M. Baranger and E. Vogt (Plenum Publ. Corp., New York) vol. 10 (1978) p. 1).

The canonical relation between the spin I and the rotational frequency ω is

$$\omega = \frac{\partial H}{\partial I}$$

Thus, in the quantum mechanical case it is natural to define

$$\hbar\omega = \frac{E_I - E_{I-2}}{[I(I+1)]^{1/2} - [(I-2)(I-1)]^{1/2}}$$

which formula is often simplified to

$$\hbar\omega = \frac{E_I - E_{I-2}}{2}$$

i.e., twice the rotational frequency is equal to the E2 transition energy.

A standard back-bending plot shows the moment of inertia $2\mathcal{J}/\hbar^2$ as a function of the squared rotational frequency. This is illustrated for ^{158}Er and ^{174}Hf in fig. 11.13. Note that while the yrast lines, E versus $I(I+1)$, look rather similar, the differences are blown up in the $\mathcal{J}$ versus ω^2 plot. Thus, ^{158}Er shows back-bending while ^{174}Hf does not.

The yrast states of ^{160}Yb and ^{164}Hf are shown in an alternative back-bending plot, I (or rather the component I_x) versus ω, in fig. 11.14. In the spin region $I = 10$–14, two $i_{13/2}$ neutrons get aligned for each nucleus. The second irregularity (up-bend) seen for ^{160}Yb at $I \approx 28$ and for ^{158}Er at